Electronic Supplementary Information

Introducing chenodeoxycholic acid coadsorbent and strong electron-withdrawing group in indoline dyes to design high-performance solar cells: a remarkably theoretical improvement

Lemin Mao,[ab] Shuopan Dun,[ab] Hehe Ren,[ab] Jiamin Jiang,[ab] Xugeng Guo,*[ab] Fuhua Huang,[ab] Panpan Heng,[ab] Li Wang,*[ab] Jinglai Zhang*[ab] and Hans Ågren*[abc]

[a]*Institute of Upconversion Nanoscale Materials, College of Chemistry and Chemical Engineering, Henan University, Kaifeng 475004, China*

[b]*Henan Center for Outstanding Overseas Scientists, Henan University, Kaifeng 475004, China*

[c]*Department of Theoretical Chemistry and Biology, Royal Institute of Technology, Stockholm SE-10691, Sweden*

*Corresponding author. *E-mail*: xgguo@henu.edu.cn (X.G.); chemwangl@henu.edu.cn (L.W.); zhangjinglai@henu.edu.cn (J.Z.); hagren@kth.se (H.Å.).

Methods

Theoretical models

Power conversion efficiency (η) of solar cell is quantified using the following formula:[1]

$$\eta = \mathrm{FF}\frac{V_{\mathrm{OC}}J_{\mathrm{SC}}}{P_{\mathrm{inc}}} \qquad (1)$$

Where V_{OC} is the open-circuit voltage, J_{SC} is the short-circuit current density, FF is the fill factor, and P_{inc} is the input power of incident solar light (taking the measurement value of 100 mW cm^{-2}).[2]

In general, J_{SC} largely depends on the light-harvesting ability including the optical absorption region and intensity of the dye, which can be evaluated using the following equation:[3]

$$J_{\mathrm{SC}} = e\int \mathrm{LHE}(\lambda)\Phi_{\mathrm{inj}}\eta_{\mathrm{reg}}\eta_{\mathrm{coll}}\varphi_{\mathrm{ph.AM1.5G}}(\lambda) \qquad (2)$$

where Φ_{inj} is the electron injection efficiency, η_{reg} is the dye regeneration efficiency, η_{coll} is the electron collection efficiency, and $\varphi_{\mathrm{ph.AM1.5G}}$ is the photon flux corresponding to the AM 1.5G solar radiation spectrum.

The LHE(λ) is the light-harvesting efficiency, which can be defined as:[4]

$$\mathrm{LHE}(\lambda) = 1 - 10^{-\varepsilon(\lambda)\Gamma} \qquad (3)$$

where $\varepsilon(\lambda)$ is the molar absorption coefficient at a certain wavelength, which can be calculated by the TD-DFT method, Γ is the amount of dye loading on the surface of TiO_2, which is taken to be 100 nmol cm^{-2} for **WS-2** and 60 nmol cm^{-2} for **WS-2a**. Such a difference in the amount of dye loading is based on the different molecular size.

The Φ_{inj} and η_{coll} values can be computed based on the following equations:

$$\Phi_{inj} = \frac{1}{1 + \tau_{inj} / \tau_{relax}} \qquad (4)$$

$$\eta_{coll} = \frac{1}{1 + \tau_{trans} / \tau_{rec}} \qquad (5)$$

where τ_{inj} represents the electron injection lifetime from the excited dye to the TiO_2 film, equal to the reciprocal of electron injection rate (k_{inj}) evaluated in the framework of the Marcus theory,[5,6] τ_{relax} is the relaxation time for the excited state of dye in solution (~10 ps based on the experimental measurements)[7], τ_{trans} is the electron transport time for electrons in TiO_2 CB toward the electrode (usually in picosecond order of magnitude), and τ_{rec} is the electron recombination lifetime, equal to the reciprocal of electron recombination rate (k_{rec}) also obtained from the Marcus theory expression. It is worthy to note that the η_{coll} almost equals to 1 owing to the extremely small k_{rec} in the present systems. Given that the Φ_{inj}, η_{reg}, and η_{coll} are arbitrarily set to 1, the maximum short-circuit current density (J_{SC}^{max}) can be obtained.

Based on Marcus theory, the nonadiabatic electron transfer rate can be estimated as follows:[5,6]

$$k_{ET} = A\sqrt{\frac{\pi}{\hbar^2 \lambda k_B T}} \exp(-\beta r) \exp\left[\frac{-(-\Delta G^0 + \lambda)^2}{4\lambda k_B T}\right] \qquad (6)$$

where A is a constant (0.025), k_B is the Boltzmann constant, T is the temperature (300 K), β is the attenuation factor (0.5 $Å^{-1}$),[8] r is the electron transfer distance, ΔG^0 is the driving force of the reaction, and λ is the total reorganization energy.

The V_{OC} can be calculated as:[9]

$$V_{OC} = \frac{k_B T}{\beta' q} \ln \frac{\beta' q R_0 J_{SC}}{k_B T} \qquad (7)$$

where β' is the charge transfer coefficient for recombination of electrons, which is taken to be 0.45, referred to the empirical value.[10] R_0 is the recombination resistance, which is calculated as:

$$R_0 = \frac{\sqrt{\pi \lambda k_B T}}{q^2 d r k_{rec} c_{ox} N_s} \exp(\gamma \frac{E_{CBM} - E_{redox}}{k_B T} + \frac{\lambda}{4 k_B T}) \qquad (8)$$

where λ is the total reorganization energy, d is the film thickness (taking the experiment value of 10 μm),[11] c_{ox} is the concentration of acceptor species (I_3^-, ~50 mmol/L), N_s is the constant related to the total number of surface states contributing to recombination (~10^5), γ is the constant related to electron trap distribution below CB (~0.3), and k_{rec} is the electron recombination rate.

According to the current density-voltage properties of solar cells, the *I-V* curve can be depicted in the presence of known J_{SC} and V_{OC}:

$$V = \frac{k_B T}{q} \ln(\frac{J_{SC} - I}{I_S} + 1) \qquad (9)$$

$$I_S = \frac{J_{SC}}{\exp(q V_{OC} / k_B T) - 1} \qquad (10)$$

where I_S denotes the reverse saturation current. By using the maximum output power divided by J_{SC} and V_{OC}, we obtained the fill factor (FF) of all systems, which is equal to the ratio of $I_{max} \times V_{max} / J_{SC} \times V_{OC}$, where I_{max} and V_{max} are maximum current and voltage, respectively.

To explore the most stable adsorption configuration of the dyes, the adsorption energy (E_{ads}) of the dye anchored on the TiO_2 surface can be defined as

$$E_{ads} = E_{dye+TiO_2} - (E_{dye} + E_{TiO_2}) \qquad (11)$$

where $E_{dye+TiO_2}$ is the total energy of dye@TiO_2 complexes, E_{TiO_2} is the energy of pure TiO_2 supercell, and E_{dye} is the energy of the isolated dye.

The total reorganization energy (λ) contains both inner-sphere (λ_i) and outer-sphere (λ_o) components; $\lambda=\lambda_i+\lambda_o$.[5,12]

The inner-sphere reorganization energy (λ_i) is the sum of hole reorganization energy (λ_h) and electron reorganization energy (λ_e), both of which can be estimated as follows.[13–15]

$$\lambda_h = (E_0^+ - E_+^+) + (E_+^0 - E_0^0) \qquad (12)$$

$$\lambda_e = (E_0^- - E_-^-) + (E_-^0 - E_0^0) \qquad (13)$$

in which E_0^+ (E_0^-) is the energy of cation (anion) calculated from the optimized structure of the neutral molecule; E_+^+ (E_-^-) is the energy of cation (anion) calculated from the optimized cation (anion) geometry; E_+^0 (E_-^0) is the energy of neutral molecule computed from the cationic (anionic) state; E_0^0 is the energy of neutral molecule at the ground state. The contribution of the outer-sphere reorganization energy (λ_o) to total reorganization energy is considered to be very small (less than 0.1 eV or less).[10,16] Accordingly, the λ_o can be set to 0.1 eV.

In addition, an excellent performance of the dyes should exhibit better charge transfer and injection capability. The ionization potential (IP) and electron affinity (EA) are used to describe the energy barrier for hole and electron injection. A smaller IP and a larger EA can lead to a better hole and electron transport, respectively. IP and EA can be estimated as the following expression:

$$\mathrm{IP} = E_0^0 - E_0^+ \qquad (14)$$

$$\mathrm{EA} = E_0^- - E_0^0 \qquad (15)$$

Computational details

In current work, no structural simplification was applied for **WS-2**, **WS-2a** and CDCA. All calculations following the ground-state geometric optimization were performed by using B3LYP[17–19] functional and 6-31G(d,p) basis set. To ensure that all the original dyes are in the most stable configurations, frequency calculations were carried out at the same level of theory to obtain the corresponding minima on the potential energy surfaces. Subsequently, we applied CAM-B3LYP[20] exchange correlation functional and 6-31G(d,p) basis set in framework of TD-DFT to describe the absorption spectra of targeted dyes. The CAM-B3LYP functional provides a good description of the intramolecular charge transfer excitations.[21–23] Solvent effects are considered by using the polarizable continuum model (PCM)[24,25] of SCRF in dichloromethane. The above-mentioned electronic calculations were performed by the Gaussian 09 program.[26]

To assess the interaction between dye and TiO_2, **WS-2** or **WS-2a** molecule was adsorbed on the anatase TiO_2(101) supercell[27] since the most stable TiO_2(101) facet has been widely employed in previous literatures to study the adsorption properties. To further study the effects of the CDCA coadsorbent on the dye@TiO_2 system, the (**WS-2**+CDCA)@TiO_2 and (**WS-2a**+CDCA)@TiO_2 were also constructed. The plane-wave DFT method built in vienna ab initio simulation package (VASP),[28,29] was employed with the generalized gradient approximation (GGA)[30] and

Perdew-Burke-Ernzerhof (PBE) functional[31] to optimize the dye@TiO_2 and (dye+CDCA)@TiO_2 systems. The single adsorption of dye and CDCA and co-adsorbent of dye+CDCA with different dye coverages was simulated using the 2×3×6, 4×3×6, and 4×4×6 surface supercells. In all calculations, the atoms belonging to the top three atomic layers of the TiO_2(101) surface slab were relaxed to their energy minima, and the remaining layers were fixed using the bulk geometry parameters. An energy cutoff of 400 eV was used and the optimization would be terminated when the force on each atom was smaller than 0.1 eV $Å^{-1}$. The Grimme D2 dispersion correction was added to the functional to take into account dispersion effects. Furthermore, the total densities of states (TDOS) of all the adsorbed systems and the projected densities of states (PDOS) of the dyes and the TiO_2 supercell were also calculated at the same level to deeply analyze the adsorption properties.

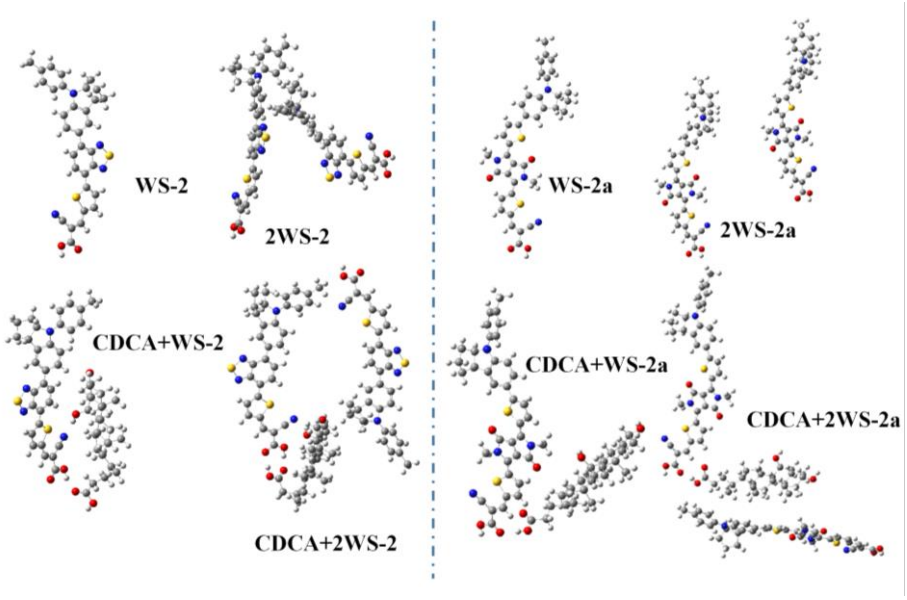

Fig. S1 Optimized geometries of dye-monomer (**WS-2** and **WS-2a**) and dye-dimer (2**WS-2** and 2**WS-2a**) forms without or with CDCA.

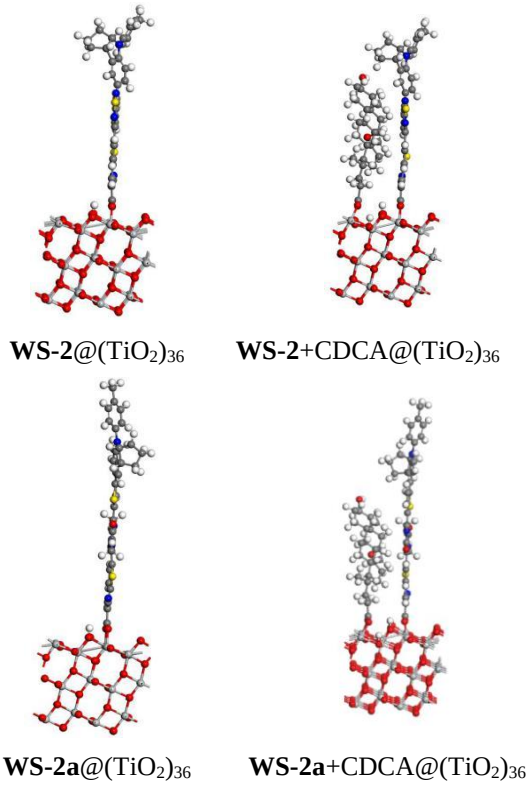

Fig. S2 Adsorption configurations for dyes **WS-2** and **WS-2a** on the anatase $(TiO_2)_{36}$ surface without or with CDCA.

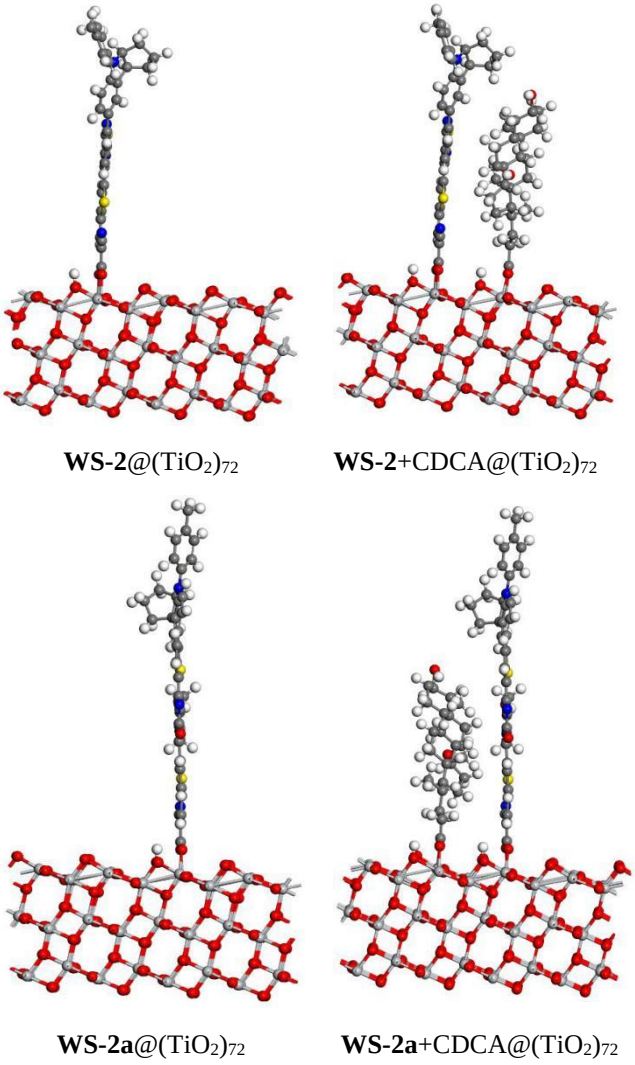

Fig. S3 Adsorption configurations for dyes **WS-2** and **WS-2a** on the anatase $(TiO_2)_{72}$ surface without or with CDCA.

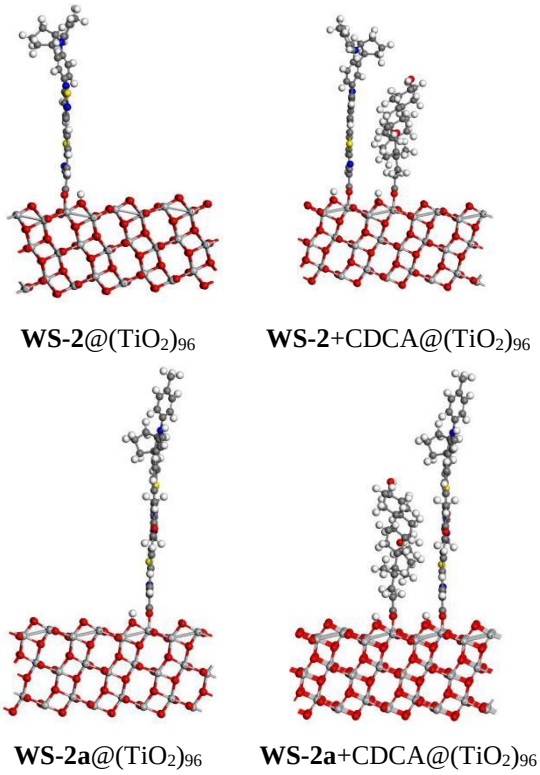

Fig. S4 Adsorption configurations for dyes **WS-2** and **WS-2a** on the anatase $(TiO_2)_{96}$ surface without or with CDCA.

Table S1 Excitation energies (eV), absorption peaks (nm), oscillator strength (*f*), major composition of MO, and major transitions

Dye	State	*E*/eV	*λ*/nm	*f*	Major composition
WS-2	S_1	2.38	522	1.2325	H→L (78%); H-1→L (13%)
	S_2	3.25	382	0.3846	H-1→L (51%); H→L+1 (31%)
WS-2+CDCA	S_1	2.41	514	1.1250	H→L (75%); H-1→L (17%)
	S_2	3.23	384	0.3210	H-1→L (56%); H →L+1 (23%)
2**WS-2**	S_1	2.36	525	1.1346	H→L+1 (76%); H-2→L+1 (12%)
	S_2	2.47	503	1.2098	H-1→L (71%); H-3→L (16%)
2**WS-2**+CDCA	S_1	2.32	535	0.4201	H→L (61%); H-1→L+1 (16%)
	S_2	2.36	525	2.1030	H-1→L+1 (61%); H→L (16%)
WS-2a	S_1	1.94	638	1.5234	H→L (76%); H-1→L (17%)
	S_2	2.86	434	0.3513	H-1→L (68%); H→L (10%)
WS-2a+CDCA	S_1	1.90	651	1.5263	H→L (76%); H-1→L (18%)
	S_2	2.82	440	0.3328	H-1→L (69%); H→L (11%)
2**WS-2a**	S_1	1.94	639	0.0453	H→L (47%); H-1→L+1 (29%)
	S_2	1.96	634	2.9590	H-1→L+1 (47%); H→L (29%)
2**WS-2a**+CDCA	S_1	1.91	648	1.5979	H→L (69%); H-2→L (15%)
	S_2	1.94	640	1.4752	H-1→L+1 (70%); H-3→L+1 (14%)

Table S2 Contour plots of HOMO and LUMO calculated at the B3LYP/6-31G(d,p) level of theory

Dye	WS-2	WS-2a
LUMO	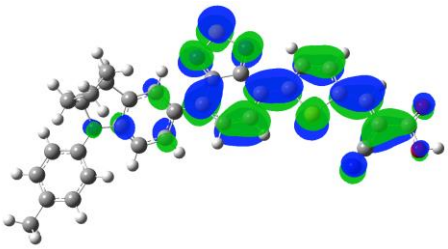	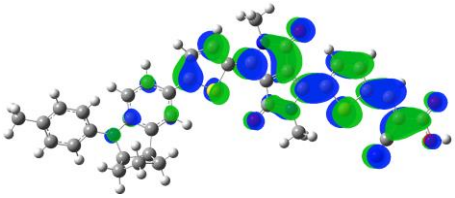
	-2.90 eV	**-3.07 eV**
Δ*E*	**2.09 eV**	**1.75 eV**
HOMO	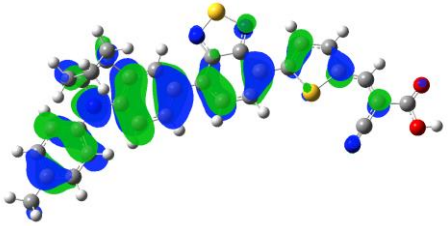	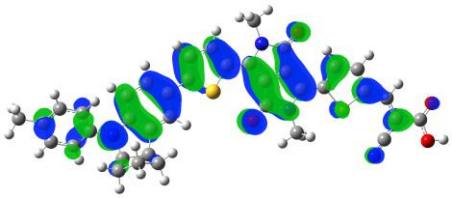
	-4.99 eV	**-4.82 eV**

Table S3 Calculated ionization energy (IP), electron affinity (EA), electron (λ_e), hole (λ_h), and total (λ_{total}) reorganization energy of dyes **WS-2** and **WS-2a** without or with CDCA

Dye	IP (eV)	EA (eV)	λ_e (eV)	λ_h (eV)	λ_{total} (eV)
WS-2	6.07	1.73	0.31	0.17	0.48
WS-2+CDCA	5.91	1.70	0.49	0.23	0.72
2**WS-2**	5.84	2.13	0.27	0.12	0.39
2**WS-2**+CDCA	5.60	2.19	0.20	0.07	0.27
WS-2a	5.78	2.00	0.28	0.23	0.51
WS-2a+CDCA	5.79	2.08	0.40	0.31	0.71
2**WS-2a**	5.46	2.38	0.25	0.17	0.42
2**WS-2a**+CDCA	5.42	2.40	0.17	0.12	0.30

Table S4 Calculated dihedral angles (in degrees) between each part of dye molecules

Dye	Donor-Auxiliary acceptor	Auxiliary acceptor-π	π-Anchor
WS-2	30.66º	1.20º	0.02º
WS-2+CDCA	34.62º	6.60º	3.46º
2**WS-2**	31.47º/37.10º	0.96º/3.55º	0.01º/0.08º
2**WS-2**+CDCA	28.30º/30.98º	5.13º/8.40º	0.52º/1.38º
WS-2a	18.41º	-0.66º	0.01º
WS-2a+CDCA	18.03º	-1.15º	0.92º
2**WS-2a**	18.07º/17.28º	-0.67º/-1.42º	-0.04º/-0.14º
2**WS-2a**+CDCA	14.90º/12.78º	-2.10º/-0.55º	-0.06º/0.27º

Table S5 Estimated electron injection distance (r_{inj}, in Å), electron recombination distance (r_{rec}, in Å), electron injection rate (k_{inj}, in s^{-1}), electron recombination rate (k_{rec}, in s^{-1}), electron injection efficiency (Φ_{inj}), electron collection efficiency (η_{coll}) and short-circuit current density (J_{SC}, in mA cm^{-2}) for dyes **WS-2** and **WS-2a** under different TiO_2 supercells with or without CDCA, along with the corresponding experimental value

TiO_2	Dye	r_{inj}	r_{rec}	k_{inj}	k_{rec}	Φ_{inj}	η_{coll}	J_{SC}	J_{SC} (expt)[a]
2×3×6	**WS-2**	2.50	17.11	1.51×10^{14}	18817498	0.9993	1.000	18.09	18.19
	WS-2+CDCA	2.53	17.17	4.21×10^{12}	6170591	0.9768	1.000	16.76	
4×3×6	**WS-2**	2.54	17.17	1.45×10^{14}	1401563	0.9993	1.000	18.09	
	WS-2+CDCA	2.53	17.19	3.61×10^{13}	652742	0.9972	1.000	17.11	
4×4×6	**WS-2**	2.48	17.00	5.16×10^{13}	114016	0.9981	1.000	18.06	
	WS-2+CDCA	2.53	17.13	1.13×10^{14}	43533	0.9991	1.000	17.14	
	2**WS-2**	2.54	17.15	5.92×10^{13}	270952	0.9983	1.000	18.98	
	2**WS-2**+CDCA	2.54	17.15	2.88×10^{13}	740558	0.9965	1.000	19.73	
2×3×6	**WS-2a**	2.55	20.68	4.72×10^{13}	4693372	0.9979	1.000	24.95	
	WS-2a+CDCA	2.55	20.68	2.70×10^{12}	4056254	0.9643	1.000	24.00	
4×3×6	**WS-2a**	2.47	20.54	1.44×10^{14}	49803	0.9993	1.000	24.98	
	WS-2a+CDCA	2.47	20.56	2.88×10^{13}	30939	0.9965	1.000	24.80	
4×4×6	**WS-2a**	2.47	20.42	1.56×10^{14}	70042	0.9994	1.000	24.98	
	WS-2a+CDCA	2.47	20.42	6.43×10^{13}	33307	0.9984	1.000	24.85	
	2**WS-2a**	2.47	20.39	1.68×10^{14}	148606	0.9994	1.000	25.80	
	2**WS-2a**+CDCA	2.47	20.44	1.65×10^{14}	1655276	0.9994	1.000	25.78	

[a] Experimental results from Ref. 2.

Table S6 Adsorption energy (E_{ads}, in eV) of the studied dyes adsorbed on the anatase $(TiO_2)_{36}$ and $(TiO_2)_{96}$ supercells and bond distance ($D_{Ti\text{-}O}$, in Å) between the O Atom of dye/CDCA and the Ti atom of TiO_2 with or without CDCA

Supercell	Dye	E_{ads}	$D_{Ti\text{-}O}$	
$(TiO_2)_{36}$	**WS-2**	–1.26	1.938	2.016
	WS-2+CDCA	–2.25	1.940	1.995
	CDCA	–0.19	1.993	2.050
	WS-2a	–1.14	1.968	2.012
	WS-2a+CDCA	–2.38	1.990	2.002
	CDCA	–0.26	1.974	2.028
$(TiO_2)_{96}$	**WS-2**	–0.35	1.981	1.986
	WS-2+CDCA	–0.11	1.967	1.978
	CDCA	–0.40	1.952	2.055
	WS-2a	–0.55	1.951	2.031
	WS-2a+CDCA	–0.97	1.940	2.031
	CDCA	–0.92	1.936	2.033

Table S7 Calculated CBM and LUMO energy levels (in eV), driving forces for electron injection (ΔG_{inj}, in eV) after adsorption on TiO_2 surface, and electron injection time (τ_e, in fs) for studied dyes

TiO_2	Dye	CBM	LUMO	ΔG_{inj}[a]
2×3×6	**WS-2**	-2.11	-1.58	0.53
	WS-2+CDCA	-1.50	-1.22	0.28
4×3×6	**WS-2**	-2.70	-2.04	0.64
	WS-2+CDCA	-2.30	-1.81	0.49
4×4×6	**WS-2**	-2.87	-2.03	0.84
	WS-2+CDCA	-2.63	-1.92	0.71
	2**WS-2**	-2.45	-1.73	0.72
	2**WS-2**+CDCA	-2.19	-1.55	0.64
2×3×6	**WS-2a**	-2.11	-1.77	0.34
	WS-2a+CDCA	-1.61	-1.37	0.24
4×3×6	**WS-2a**	-2.82	-2.28	0.54
	WS-2a+CDCA	-2.56	-2.11	0.45
4×4×6	**WS-2a**	-2.99	-2.37	0.62
	WS-2a+CDCA	-2.76	-2.20	0.56
	2**WS-2a**	-2.50	-1.96	0.54
	2**WS-2a**+CDCA	-2.31	-1.83	0.48

[a] Driving force for electron injection $\Delta G_{inj} = E_{LUMO} - E_{CBM}$.

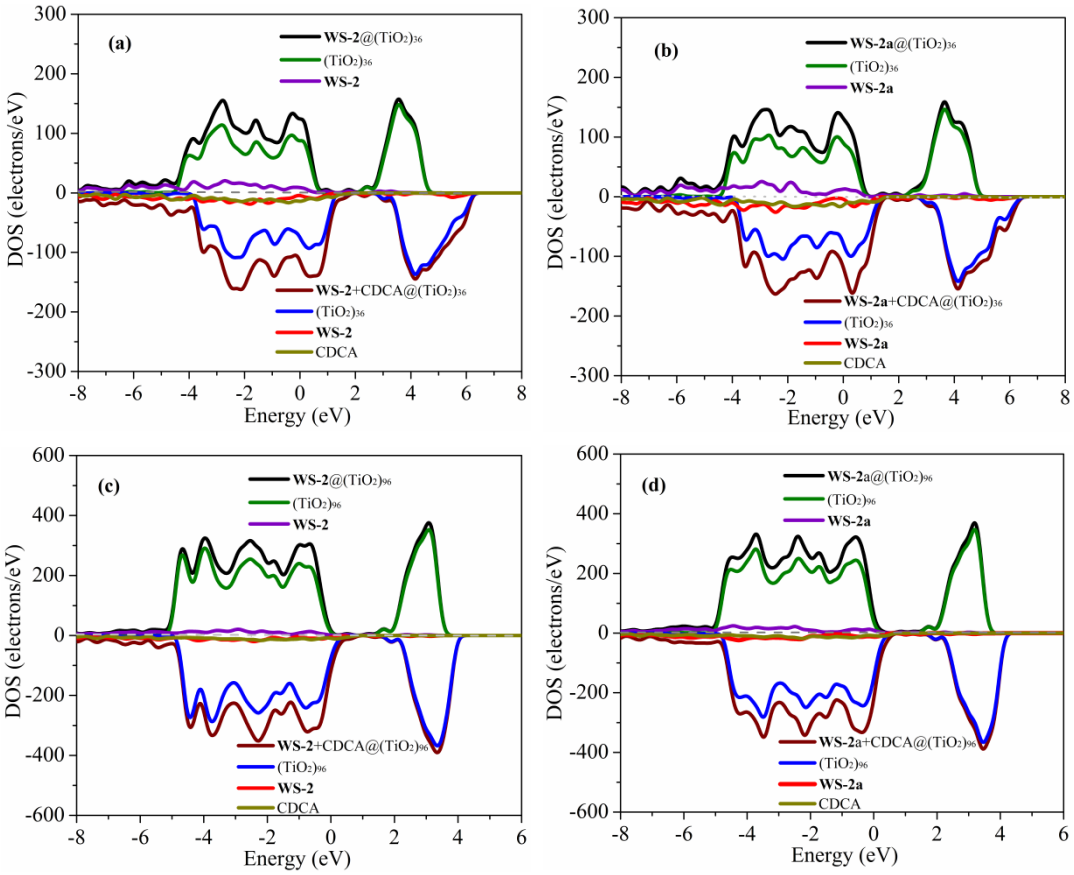

Fig. S5 Aligned DOS and PDOS of **WS-2** (a,c) and **WS-2a** (b,d) adsorbed on the $(TiO_2)_{36}$ and $(TiO_2)_{96}$ supercells with or without CDCA.

Table S8 Photophysical and photovoltatic performances of DSSCs based on indoline-containing D-A-π-A type organic dyes

Dye	CT band/nm	$E_{0\text{-}0}$/eV	J_{SC}/mA cm^{-2}	V_{OC}/mV	FF	η/%	Ref.
WS-1	496[a]	2.06	11.9	650	0.68	5.3	32
WS-5	496[b]	2.12	13.18	780	0.78	8.02	33
WS-6	547[b]	2.06	15.00	672	0.77	7.76	34
WS-8	495[b]	2.09	13.39	680	0.74	6.74	33
WS-9	536[b]	2.05	18.00	696	0.72	9.04	35
WS-11	557[b]	1.85	10.4	629	0.71	4.64	34
WS-13	505[b]	2.15	12.20	705	0.75	6.45	36
WS-22	518[b]	2.01	13.77	615	0.705	5.97	37
WS-23	545[b]	1.87	16.91	672	0.717	8.15	37
WS-24	551[a]	1.79	13.35	671	0.693	6.21	38
WS-26	552[a]	1.83	17.84	709	0.681	8.61	38
WS-51	551[a]	1.83	19.69	700	0.731	10.08	39
WS-52	549[b]	2.02	7.88	640	0.68	3.44	40
WS-53	570[b]	1.89	1.22	440	0.48	0.22	40
WS-54	563[b]	1.83	15.84	660	0.68	7.14	40
WS-55	558[b]	1.77	19.66	678	0.70	9.46	40
LS-2	442[b]	2.30	10.06	748	0.68	5.11	41
I-3	491[c]	2.05	11.63	639	0.68	5.08	42
S3	433[b]	2.05	8.23	727	0.71	4.26	43
YCD01	526[b]	-	13.40	760	0.73	7.43	44
YS04	385[d]	2.53	5.10	772	0.732	2.88	45
YS01	386[d]	2.48	8.23	767	0.735	4.64	45

[a] In $CHCl_3$+MeOH; [b] In CH_2Cl_2; [c] In CH_3CN+CH_2Cl_2; [d] In DMF.

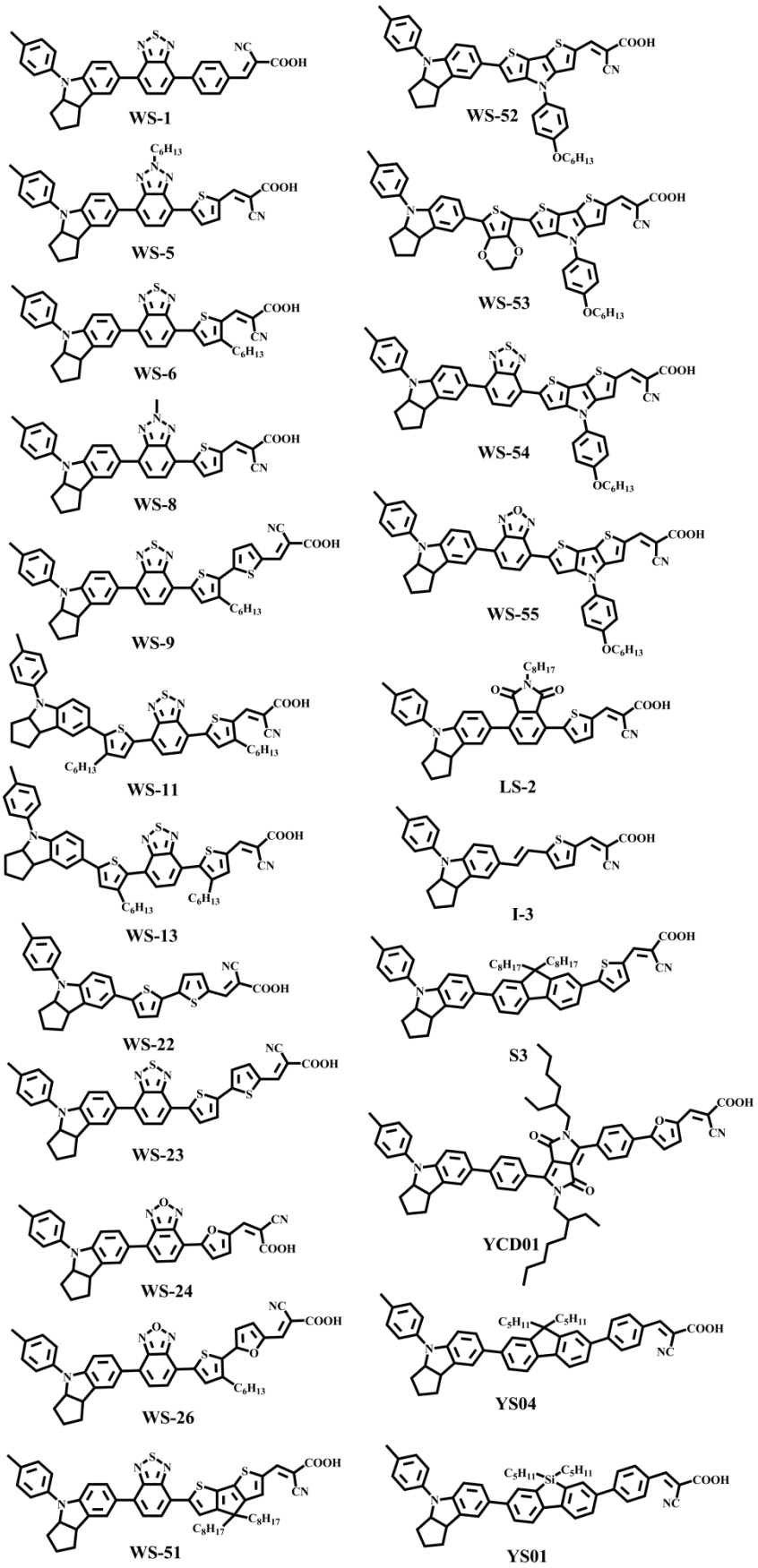

Fig. S6 Chemical structures of indoline-based dyes.

Notes and references

1 M. Grätzel, Recent advances in sensitized mesoscopic solar cells, *Acc. Chem. Res.*, 2009, **42**, 1788-1798.

2 W. Zhang, Y. Wu, H. Zhu, Q. Chai, J. Liu, H. Li, X. Song and W.-H. Zhu, Rational molecular engineering of indoline-based D-A-π-A organic sensitizers for long-wavelength-responsive dye-sensitized solar cells, *ACS Appl. Mater. Inter.*, 2015, **7**, 26802-26810.

3 J. W. Ondersma and T. W. Hamann, Recombination and redox couples in dye-sensitized solar cells, *Coord. Chem. Rev.*, 2013, **257**, 1533-1543.

4 N. Vlachopoulos, P. Liska, J. Augustynski and M. Grätzel, Very efficient visible light energy harvesting and conversion by spectral sensitization of high surface area polycrystalline titanium dioxide films, *J. Am. Chem. Soc.*, 1988, **110**, 1216-1220.

5 R. A. Marcus, On the theory of oxidation-reduction reactions involving electron transfer, *J. Chem. Phys.*, 1956, **24**, 966-978.

6 T. J. Meade, H. B. Gray and J. R. Winkler, Driving-force effects on the rate of long-range electron transfer in ruthenium-modified cytochrome c, *J. Am. Chem. Soc.*, 1989, **111**, 4353-4356.

7 N. J. Cherepy, G. P. Smestad, M. Grätzel and J. Z. Zhang, Ultrafast electron injection: implications for a photoelectrochemical cell utilizing an anthocyanin dye-sensitized TiO_2 nanocrystalline electrode, *J. Phys. Chem. B*, 1997, **101**, 9342-9351.

8 J. Wiberg, T. Marinado, D. P. Hagberg, L. Sun, A. Hagfeldt and B. Albinsson,

Distance and driving force dependencies of electron injection and recombination dynamics in organic dye-sensitized solar cells, *J. Phys. Chem. B*, 2010, **114**, 14358-14363.

9 S. R. Raga, E. M. Barea and F. Fabregat-Santiago, Analysis of the origin of open circuit voltage in dye solar cells, *J. Phys. Chem. Lett.*, 2012, **3**, 1629-1634.

10 P. Ren, C. Sun, Y. Shi, P. Song, Y. Yang and Y. Li, Global performance evaluation of solar cells using two models: from charge-transfer and recombination mechanisms to photoelectric properties, *J. Mater. Chem. C*, 2019, **7**, 1934-1947.

11 D. P. Hagberg, T. Marinado, K. M. Karlsson, K. Nonomura, P. Qin, G. Boschloo, T. Brinck, A. Hagfeldt and L. Sun, Tuning the HOMO and LUMO energy levels of organic chromophores for dye sensitized solar cells, *J. Org. Chem.*, 2007, **72**, 9550-9556.

12 N. S. Hush, Adiabatic rate processes at electrodes. I. energy charge relationships, *J. Chem. Phys.*, 1958, **28**, 962-972.

13 S. T. Bromley, M. M. Torrent, P. Hadley and C. Rovira, Importance of intermolecular interactions in assessing hopping mobilities in organic field effect transistors: pentacene versus dithiophene-tetrathiafulvalene, *J. Am. Chem. Soc.*, 2004, **126**, 6544-6545.

14 M. M. Torrent, P. Hadley, S. T. Bromley, X. Ribas, J. Tarre, M. Mas, E. Molins, J. Veciana and C. Rovira, Correlation between crystal structure and mobility in organic field-effect transistors based on single crystals of tetrathiafulvalene derivatives, *J. Am. Chem. Soc.*, 2004, **126**, 8546-8553.

15 J. Cornil, J. P. Calbert and J. L. Bredas, Electronic structure of the pentacene single crystal: relation to transport properties, *J. Am. Chem. Soc.*, 2001, 123, 4356-4361.

16 K. Schmidt, S. Brovelli, V. Coropceanu, D. Beljonne, J. Cornil, C. Bazzini, T. Caronna, R. Tubino, F. Meinardi, Z. Shuai and J. L. Brédas, Intersystem crossing processes in nonplanar aromatic heterocyclic molecules, *J. Phys. Chem. A*, 2007, **111**, 10490-10499.

17 C. Lee, ; W. Yang and R. G. Parr, Development of the colic-salvetti correlation-energy formula into a functional of the electron density, *Phys. Rev. B*, 1988, **37**, 785-789.

18 A. D. Becke, Density-functional thermochemistry. III. The role of exact exchange, *J. Chem. Phys*., 1993, **98**, 5648-5652.

19 B. Miehlich, A. Savin, H. Stoll and H. Preuss, Results obtained with the correlation energy density functionals of Becke and Lee, Yang and Parr, *Chem. Phys. Lett*., 1989, **157**, 200-206.

20 T. Yanai, D. P. Tew and N. C. Handy, A new hybrid exchange-correlation functional using the coulomb-attenuating method (CAM-B3LYP), *Chem. Phys. Lett*., 2004, **393**, 51-57.

21 D. Jacquemin, E. A. Perpète, G. E. Scuseria, I. Ciofini and C. Adamo, TD-DFT performance for the visible absorption spectra of organic dyes: conventional versus long-range hybrids, *J. Chem. Theory Comput.*, 2008, **4**, 123-135.

22 X. Guo and Z. Cao, Low-Lying electronic states and their nonradiative deactivation of thieno[3,4-b]pyrazine: an ab initio study, *J. Chem. Phys.*, 2012, **137**,

224313.

23 X. Shi, Y. Yang, L. Wang and Y. Li, Introducing asymmetry induced by benzene substitution in a rigid fused π spacer of D-π-A-type solar cells: a computational investigation, *J. Phys. Chem. C*, 2019, **123**, 4007-4021.

24 E. Cancès, B. Mennucci and J. A Tomasi, A new integral equation formalism for the polarizable continuum model: theoretical background and applications to isotropic and anisotropic dielectrics, *J. Chem. Phys*., 1997, **107**, 3032-3041.

25 M. Cossi, V. Barone, B. Mennucci and J. Tomasi, Ab initio study of ionic solutions by a polarizable continuum dielectric model, *Chem. Phys. Lett*., 1998, **286**, 253-260.

26 M. J. Frisch, G. W. Trucks, H. B. Schlegel, G. E. Scuseria, M. A. Robb, J. R. Cheeseman, G. Scalmani, V. Barone, B. Mennucci, G. A. Petersson, et al. *Gaussian 09*, Revision C.01; Gaussian, Inc.: Wallingford CT, 2010.

27 A. Vittadini, A. Selloni, F. P. Rotzinger and M. Grätzel, Structure and energetics of water adsorbed at TiO2 anatase (101) and (001) surfaces, *Phys. Rev. Lett.*, 1998, **81**, 2954-2957

28 G. Kresse and J. Furthmüller, Efficient iterative schemes for ab initio total-energy calculations using a plane-wave basis set, *Phys. Rev. B*, 1996, **54**, 11169-11186.

29 G. Kresse and J. Furthmüller, Efficiency of ab-initio total energy calculations for metals and semiconductors using a plane-wave basis set, *Comp. Mater. Sci*., 1996, **6**, 15-50.

30 J. P. Perdew, K. Burke and M. Ernzerhof, Generalized gradient approximation

made simple, *Phys. Rev. Lett*., 1996, **77**, 3865-3868.

31 R. Elmér, M.Berg, L. Carlén, B. Jakobsson, B. Norén, A. Oskarsson, G. Ericsson, J. Julien, T. F. Thorsteinsen, M. Guttormsen, G. Løvhøiden, V. Bellini, E. Grosse, C. Müntz, P. Senger and L. Westerberg, K^+ emission in symmetric heavy ion reactions at subthreshold energies, *Phys. Rev. Lett*., 1996, **77**, 4884-4886.

32 W. Zhu, Y. Wu, S. Wang, W. Li, X. Li, J. Chen, Z. Wang and H. Tian, Organic D-A-π-A solar cell sensitizers with improved stability and spectral response, *Adv. Funct. Mater.*, 2011, **21**, 756-763.

33 Y. Cui, Y. Wu, X. Lu, X. Zhang, G. Zhou, F. B. Miapeh, W. Zhu and Z.-S. Wang, Incorporating benzotriazole moiety to construct D-A-π-A organic sensitizers for solar cells: significant enhancement of open-circuit photovoltage with long alkyl group, *Chem. Mater.*, 2011, **23**, 4394-4401.

34 Y. Wu, X. Zhang, W. Li, Z.-S. Wang, H. Tian and W. Zhu, Hexylthiophene-featured D-A-π-A structural indoline chromophores for coadsorbent-free and panchromatic dye-sensitized solar cells, *Adv. Energy Mater.*, 2012, **2**, 149-156.

35 Y. Wu, M. Marszalek, S. M. Zakeeruddin, Q. Zhang, H. Tian, M. Grätzel and W. Zhu, High-conversion-efficiency organic dye-sensitized solar cells: molecular engineering on D-A-π-A featured organic indoline dyes, *Energy Environ. Sci*., 2012, **5**, 8261-8272.

36 Y. Wu and W. Zhu, Organic sensitizers from D-π-A to D-A-π-A: effect of the internal electron-withdrawing units on molecular absorption, energy levels and

photovoltaic performances, *Chem. Soc. Rev.,* 2013, **42**, 2039-2058.

37 H. Zhu, W. Li, Y. Wu, B. Liu, S. Zhu, X. Li, H. Ågren and W. Zhu, Insight into benzothiadiazole acceptor in D-A-π-A configuration on photovoltaic performances of dye-sensitized solar cells, *ACS Sustainable Chem. Eng.*, 2014, **2**, 1026-1034.

38 H. Zhu, Y. Wu, J. Liu, W. Zhang, W. Wu and W.-H. Zhu, D-A-π-A featured sensitizers containing an auxiliary acceptor of benzoxadiazole: molecular engineering and co-sensitization, *J. Mater. Chem. A*, 2015, **3**, 10603-10609.

39 Q. Chai, W. Li, J. Liu, Z. Geng, H. Tian and W.-H. Zhu, Rational molecular engineering of cyclopentadithiophene-bridged D-A-π-A sensitizers combining high photovoltaic efficiency with rapid dye adsorption, *Sci. Rep*., 2015, **5**, 11330.

40 Y. Xie, W. Wu, H. Zhu, J. Liu, W. Zhang, H. Tian and W.-H. Zhu, Unprecedentedly targeted customization of molecular energy levels with auxiliary-groups in organic solar cell sensitizers, *Chem. Sci.*, 2016, **7**, 544-549.

41 W. Li, Y. Wu, Q. Zhang, H. Tian and W. Zhu, D-A-π-A featured sensitizers bearing phthalimide and benzotriazole as auxiliary acceptor: effect on absorption and charge recombination dynamics in dye-sensitized solar cells, *ACS Appl. Mater. Inter.*, 2012, **4**, 1822-1830.

42 B. Liu, Q. Liu, D. You, X. Li and Y. Narutac and W. Zhu, Molecular engineering of indoline based organic sensitizers for highly efficient dye-sensitized solar cells, *J. Mater. Chem.*, 2012, **22**, 13348-13356.

43 W. Li, Y. Wu, X. Li, Y. Xie and W. Zhu, Absorption and photovoltaic properties of organic solar cell sensitizers containing fluorene unit as conjunction bridge, *Energy*

Environ. Sci., 2011, 4, 1830-1837.

44 S. Qu, C. Qin, A. Islam, Y. Wu, W. Zhu, J. Hua, H. Tian and L. Han, A novel D-A-π-A organic sensitizer containing a diketopyrrolopyrrole unit with a branched alkyl chain for highly efficient and stable dye-sensitized solar cells, *Chem. Commun.*, 2012, **48**, 6972-6974.

45 M. Akhtaruzzaman, Y. Seya, N. Asao, A. Islam, E. Kwon, A. El-Shafei, L. Han and Y. Yamamoto, Donor-acceptor dyes incorporating a stable dibenzosilole π-conjugated spacer for dye-sensitized solar cells, *J. Mater. Chem.*, 2012, **22**, 10771-10778.